Journal of Quantitative Spectroscopy & Radiative Transfer 186 (2017) 139–149

Contents lists available at ScienceDirect

Journal of Quantitative Spectroscopy & Radiative Transfer

journal homepage: www.elsevier.com/locate/jqsrt

New and improved infra-red absorption cross sections and ACE-FTS retrievals of carbon tetrachloride (CCl_4)

Jeremy J. Harrison [a,b,*], Christopher D. Boone [c], Peter F. Bernath [c,d]

[a] Department of Physics and Astronomy, University of Leicester, Leicester LE1 7RH, United Kingdom
[b] National Centre for Earth Observation, University of Leicester, Leicester LE1 7RH, United Kingdom
[c] Department of Chemistry, University of Waterloo, Waterloo, Ontario, Canada N2L 3G1
[d] Department of Chemistry and Biochemistry, Old Dominion University, Norfolk, Virginia 23529, United States of America

ARTICLE INFO

Article history:
Received 17 February 2016
Received in revised form
28 April 2016
Accepted 28 April 2016
Available online 6 May 2016

Keywords:
CCl_4
Carbon tetrachloride
High-resolution Fourier transform spectroscopy
Infra-red absorption cross sections
Remote sensing
Atmospheric chemistry

ABSTRACT

Carbon tetrachloride (CCl_4) is one of the species regulated by the Montreal Protocol on account of its ability to deplete stratospheric ozone. As such, the inconsistency between observations of its abundance and estimated sources and sinks is an important problem requiring urgent attention (Carpenter et al., 2014) [5]. Satellite remote-sensing has a role to play, particularly limb sounders which can provide vertical profiles into the stratosphere and therefore validate stratospheric loss rates in atmospheric models.

This work is in two parts. The first describes new and improved high-resolution infra-red absorption cross sections of carbon tetrachloride/dry synthetic air over the spectral range 700–860 cm^{-1} for a range of temperatures and pressures (7.5–760 Torr and 208–296 K) appropriate for atmospheric conditions. This new cross-section dataset improves upon the one currently available in the HITRAN and GEISA databases. The second describes a new, preliminary ACE-FTS carbon tetrachloride retrieval that improves upon the v3.0/v3.5 data products, which are biased high by up to ~20–30% relative to ground measurements. Making use of the new spectroscopic data, this retrieval also improves the microwindow selection, contains additional interfering species, and utilises a new instrumental lineshape; it will form the basis for the upcoming v4.0 CCl_4 data product.

1. Introduction

A clear, colourless, sweet-smelling liquid at room temperature, carbon tetrachloride (CCl_4; also known as tetrachloromethane or CFC-10) was first synthesised in 1839 from chloroform and chlorine gas by Henry Victor Regnault [1]. As carbon tetrachloride does not occur naturally in the Earth system, its presence in the atmosphere, soil and ocean arises through its anthropogenic uses.

In the early twentieth century, carbon tetrachloride found many uses, for example in dry cleaning (excellent solvent properties), fire extinguishers, postage stamp collecting (to reveal watermarks without damaging the paper), lava lamps, and even as a refrigerant in early refrigerators. The discovery that carbon tetrachloride is harmful to human health – a potential human carcinogen, it has been shown to depress the central nervous system, inhibit liver and kidney function, and even kill – led to a decline in these uses. However, this had no effect on the largest industrial application of carbon tetrachloride in the twentieth century, its use as a feedstock in the production of trichlorofluoromethane (CFC-11) and dichlorodifluoromethane (CFC-12), which were commercialised in the 1930s as nonflammable and non-toxic refrigerants [2].

* Corresponding author at: Department of Physics and Astronomy, University of Leicester, University Road, Leicester LE1 7RH, United Kingdom.
E-mail address: jh592@leicester.ac.uk (J.J. Harrison).

http://dx.doi.org/10.1016/j.jqsrt.2016.04.025
0022-4073/

It was not until the realisation that long-lived chlorine-containing species such as CCl_4 and the CFCs (chlorofluorocarbons) could destroy stratospheric ozone that the use of CCl_4 in industry began to decline, as regulated by the 1987 Montreal Protocol (and its later amendments). Under the terms of the Protocol production and consumption of CCl_4 were eliminated for developed countries in 1996 and for developing countries in 2010 [3]. There are no limits on the use of CCl_4 as a feedstock, however, so it is still used, for example, in the production of hydrofluorocarbons. Although an ozone-depleting substance, with an ozone depletion potential of 0.72 [4], CCl_4 is also a very strong greenhouse gas with a 100-year global warming potential of 1730 [4].

As one of the species controlled by the Montreal Protocol, there is much work carried out in monitoring CCl_4 atmospheric concentrations by global networks such as AGAGE (Advanced Global Atmospheric Gases Experiment), NOAA (National Oceanic and Atmospheric Administration), and UCI (University of California, Irvine). The latest ozone assessment report from 2014 [5] indicates that the global surface mean mole fraction of CCl_4 has continued to decline between 2008 and 2012, with the AGAGE and UCI networks reporting a rate of decline of 1.2–1.3% from 2011 to 2012, and 1.6% reported by the NOAA network. These rates of decline are comparable with those determined by remote sensing instruments of 1.1–1.2% yr^{-1}, from the Atmospheric Chemistry Experiment-Fourier transform spectrometer (ACE-FTS) on SCISAT and the ground-based FTS at Jungfraujoch [6].

Recently there has been particular interest in carbon tetrachloride, on account of the inconsistency between observations of its abundance and estimated sources and sinks [3]. A recent study [3] has suggested that the observed inter-hemispheric gradient for CCl_4 (1.5 ± 0.2 ppt for 2000–2012) is primarily caused by ongoing emissions, however the 2007–2012 emissions estimate based on the UNEP reported production and feedstock usage is near-zero. Additionally, the decline of atmospheric concentrations is slower than can be accounted for by our current best estimates of the total CCl_4 lifetime and its uncertainties.

In addition to the ground-based networks of CCl_4 measurements, remote-sensing measurements which provide vertical profiles into the stratosphere are particularly useful in validating stratospheric loss rates in atmospheric models (the atmospheric loss of CCl_4 is essentially all due to photolysis in the stratosphere). The literature reports a number of remote-sensing instruments capable of measuring CCl_4 in the Earth's atmosphere: ATMOS (Atmospheric Trace MOlecule Spectroscopy) [7] and CIRRIS 1A (Cryogenic Infra-Red Radiance Instrumentation for Shuttle) [8], both deployed on the space shuttle, the JPL balloon-borne MkIV interferometer [1], MIPAS (Michelson Interferometer for Passive Atmospheric Sounding) on ENVISAT (ENVIronmental SATellite) (e.g. [9]), and the ACE-FTS [1,10].

In the literature, the only global distribution of CCl_4 extending up to the mid-stratosphere is derived from ACE-FTS measurements. Covering the spectral region 750–4400 cm^{-1} with a resolution of 0.02 cm^{-1}, the ACE-FTS instrument uses the sun as a light source to record limb transmission through the Earth's atmosphere (~300 km effective length) during sunrise and sunset ('solar occultation'). The measured spectra, with high signal-to-noise ratios and through long atmospheric path lengths, provide a low detection threshold for retrieving the profiles of trace species. In fact, the ACE-FTS can detect more of these species than any other satellite instrument, although it only records spectra for at most 30 occultation events per day [11,12 (this issue)]. Unfortunately, the ACE-FTS v3.0/v3.5 CCl_4 retrieval is biased high by up to ~20–30% relative to ground measurements; the reasons for this have been attributed to errors in the CCl_4 spectroscopy, bad line parameters from other absorbing species in the microwindow, and several absorbing species missing from the forward model. The aim of the present work was to improve the ACE-FTS CCl_4 retrieval and minimise this high bias. This problem has been attacked on two fronts: (1) through the utilisation of new laboratory spectroscopic measurements of air-broadened CCl_4 samples over a range of atmospheric pressure-temperature (PT) combinations and; (2) through improvements in the retrieval itself, in particular improved microwindow selection (the avoidance of spectral regions associated with poor or inadequate line parameters of interfering species), the inclusion of new interfering species, and a new instrumental lineshape (ILS). This new scheme will form the basis for the upcoming processing version 4.0 of ACE-FTS data. Section 2 of this manuscript presents some spectroscopic background to CCl_4, and a discussion of previous infra-red (IR) absorption cross section datasets. Section 3 provides details on the new measurements, the derivation of cross sections, and a discussion of the results and comparison with previous measurements. Section 4 provides details of the new ACE-FTS CCl_4 retrieval scheme.

2. Infra-red spectroscopy of carbon tetrachloride

2.1. Spectroscopic background

Since carbon and chlorine each have two stable isotopes, there are ten stable isotopologues of carbon tetrachloride, namely $^{12/13}C^{35}Cl_4$, $^{12/13}C^{35}Cl_3^{37}Cl$, $^{12/13}C^{35}Cl_2^{37}Cl_2$, $^{12/13}C^{35}Cl^{37}Cl_3$, and $^{12/13}C^{37}Cl_4$; these belong to the point groups T_d, C_{3v}, C_{2v}, C_{3v} and T_d, respectively. With natural abundances of ~99% and ~1% for ^{12}C and ^{13}C, and ~76% and ~24% for ^{35}Cl and ^{37}Cl, it turns out that the four isotopologues $^{12}C^{35}Cl_4$, $^{12}C^{35}Cl_3^{37}Cl$, $^{12}C^{35}Cl_2^{37}Cl_2$, and $^{12/13}C^{35}Cl^{37}Cl_3$ account for ~99% of the isotopologues found, that is 33%, 42%, 20% and 4%, respectively [13].

CCl_4 has nine normal vibrational modes; in the T_d point group these are labelled ν_1 (non-degenerate, A_1), ν_2 (doubly-degenerate, E), ν_3 (triply degenerate, T_2), and ν_4 (triply degenerate, T_2). For the lower-symmetry isotopologues, the degeneracy can be lifted; ν_2 splits into A_1 and A_2 for C_{2v}, and ν_3 and ν_4 split into A_1 and E under C_{3v}, and A_1, B_1 and B_2 under C_{2v}. In the literature, however, it is more common to label bands under the assumption of T_d symmetry, as the splittings are likely small to a first approximation.

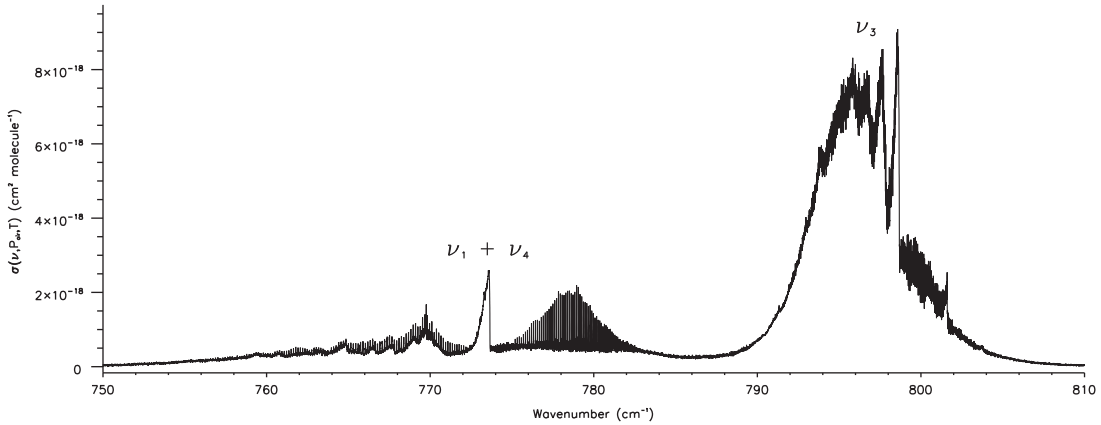

Fig. 1. The IR absorption cross section of carbon tetrachloride/dry synthetic air at 208.0 K and 7.501 Torr, with vibrational band assignments for the two main band systems in the 700–860 cm^{-1} spectral region.

The strong ν_3 fundamental and $\nu_1+\nu_4$ combination bands of CCl_4 are situated in the 700–860 cm^{-1} spectral region, with Fermi resonance between these levels resulting in both bands having mixed character and the latter having enhanced intensity [13]. The extremely dense rotation–vibration spectrum is complicated by the presence of isotopologues, which contribute to the spectrum in proportion with their natural abundances. As such, it is a difficult task to derive spectroscopic line parameters for CCl_4. For this reason, remote-sensing of the Earth's atmosphere requires the use of absorption cross sections derived from air-broadened spectra recorded in the laboratory. Fig. 1 provides a plot of the new absorption cross section at 208.0 K and 7.501 Torr with these main band systems labelled. Full details on the measurement conditions and derivation of this cross section are given in Section 3.

2.2. A brief history of carbon tetrachloride absorption crosssections

The HITRAN 1986 compilation [14] included for the first time high resolution (0.03 cm^{-1}) cross sections for the simulation of the spectra of a number of important atmospheric molecules, including CCl_4, for which no line parameters were available. These cross sections, with a quoted accuracy of 10–25%, were derived from laboratory absorption spectra of pure samples recorded at 296 K at the University of Denver [15].

The first published temperature-dependent CCl_4 cross sections appeared in 1992 [16]. Derived from measurements of pure CCl_4 at 0.05 cm^{-1} resolution and 223, 248, 273 and 298 K, these data were later included in the HITRAN 1996 compilation [17].

N_2-broadened CCl_4 absorption cross sections between 750 and 812 cm^{-1}, derived from measurements over a range of temperatures down to 208 K at a spectral resolution of 0.03 cm^{-1} [18], henceforth referred to as the Nemtchinov dataset, were subsequently included in HITRAN 2000 [19]. This dataset has been used extensively for remote-sensing applications over the last decade and a half. This dataset has remained unchanged for subsequent HITRAN compilations, including the most recent HITRAN 2012 [20], and has additionally been included in the most recent GEISA 2003 [21] and 2009 [22] compilations. Despite its widespread use, the Nemtchinov dataset has a number of deficiencies which will be fully discussed in Section 3. Such deficiencies in the underlying laboratory spectroscopy compromise the accuracy of retrieved quantities, such as volume mixing ratios (VMRs), in remote-sensing applications. The new spectroscopic dataset described in the present work provides an improvement over previous available datasets.

3. New absorption cross sections of air-broadened carbon tetrachloride

3.1. Experimental

The experimental setup and procedures have been used previously for related measurements (e.g. [23,24]), so only brief details are provided here. All measurements were performed at the Molecular Spectroscopy Facility (MSF), Rutherford Appleton Laboratory (RAL), using a Bruker Optics IFS 125 HR FTS, and an internally mounted 26-cm-pathlength sample cell connected to a Julabo F95-SL Ultra-Low Refrigerated Circulator filled with ethanol. The cell temperature was monitored by four platinum resistance thermometers (PRTs) in thermal contact at different points on the exterior surface of the cell. Mixture pressures were measured using Baratron capacitance manometers (MKS). Samples were provided by Fluka (CCl_4; analytical standard, $\geq$99.95% purity, natural-abundance isotopic mixture) and BOC Gases (dry synthetic air or 'Air Zero', total hydrocarbons $<$ 3 ppm, $H_2O < 2$ ppm, $CO_2 < 1$ ppm, $CO < 1$ ppm). The carbon tetrachloride sample (liquid at room temperature) was freeze-pump-thaw purified multiple times prior to use, whereas the synthetic air was used 'as is'. Air-broadened CCl_4 IR spectra were recorded over a range of pressures and temperatures, and at resolutions between 0.01 and 0.03 cm^{-1} (defined as the Bruker instrument resolution of 0.9/MOPD; MOPD=maximum optical path difference), 0.01 cm^{-1} for the lowest

pressures (in the Doppler-limited regime), and 0.03 cm^{-1} for the highest pressures. Pure nitrous oxide (N_2O) spectra were additionally recorded at each temperature to calibrate the wavenumber scale of the air-broadened CCl_4 spectra. The FTS instrumental parameters and settings are summarised in Table 1, with sample pressures, temperatures, and their experimental uncertainties and associated spectral resolutions listed in Table 2.

3.2. Generation of absorption cross sections

The procedure for generating absorption cross sections from experimental data has been reported previously (e.g. [23,24]). After generation of transmittance spectra from measured interferograms, the wavenumber scale is calibrated against the positions of isolated N_2O absorption lines taken from the HITRAN 2012 database [20]. Next, using a successful approach developed previously (e.g. [23,24]), absorption cross sections are derived and calibrated against a "calibration standard" integrated band strength. This is necessary to counter problems with carbon tetrachloride adsorption in the vacuum line and on the cell walls, resulting in its partial pressure during each measurement differing from the initial, measured value.

Previous absorption cross sections created for ACE-FTS retrievals have had their integrated band strengths calibrated using data from the Pacific Northwest National Laboratory (PNNL) IR database (http://nwir.pnl.gov) [25]. However, data from the National Institute of Standards and Technology (NIST) Quantitative Infra-red Database (http://webbook.nist.gov/chemistry/quant-ir/) [26] are also suitable as calibration standards. Surprisingly, it was found that for carbon tetrachloride, the NIST integrated band strength (between 700 and 860 cm^{-1}) is 5.4% higher than that for PNNL. The main difference between the CCl_4 spectra in the two databases is that the NIST measurements were made using flow-through samples in a White cell, with the PNNL measurements employing a static sample cell. For the purposes of the ACE-FTS retrievals in Section 4, it was found that calibrating to the NIST intensities resulted in a better agreement with ground-based measurements. Therefore, the absolute intensity of the absorption cross sections, $\sigma(\upsilon,P_{air},T)$, at wavenumber υ (cm^{-1}), temperature T (K) and synthetic air pressure P_{air}, was calibrated according to

$$\int_{700\ cm^{-1}}^{860\ cm^{-1}} \sigma(\upsilon,\ P_{air},\ T)\partial\upsilon = 6.7163 \times 10^{-17}\ \text{cm molecule}^{-1}, \quad (1)$$

where the value on the right hand side is the integrated band intensity over the spectral range 700–860 cm^{-1} for the composite 760-Torr-N_2-broadened CCl_4 NIST spectrum at 296 K.

3.3. Absorption cross section uncertainties

The wavenumber accuracy, i.e. uncertainty in x, of the new absorption cross sections is comparable to the accuracy of the N_2O lines used in the calibration; HITRAN error codes indicate this is between 0.001 and 0.0001 cm^{-1}.

Since only one spectrum is recorded at each PT combination, due to time constraints, it is not possible to obtain an estimate of the y-axis random errors. However, systematic errors are believed to make the dominant contribution to the uncertainty in y. Maximum uncertainties in the sample temperatures (μ_T) and total pressures (μ_P) are 0.2% and 0.8%, respectively (Table 2). The photometric uncertainty (μ_{phot}) is estimated to be ~2%. The pathlength error (μ_{path}) is estimated to be negligibly small, lower than 0.1%. The systematic error, μ_{NIST}, in the NIST CCl_4 spectrum used for intensity calibration is 2.1%. Assuming that the error estimates for all quantities are uncorrelated, the overall systematic error in the dataset

Table 1
FTS parameters and cell configuration for all measurements.

Mid-IR source	Globar
Detector	Mercury cadmium telluride (MCT) D313 [a]
Beam splitter	Potassium bromide (KBr)
Optical filter	~700–1700 cm^{-1} bandpass
Spectral resolution	0.01 to 0.03 cm^{-1}
Aperture size	3.15 mm
Apodisation function	Boxcar
Phase correction	Mertz
Cell windows	Potassium bromide (KBr) (wedged)
Pressure gauges	3 MKS-690A Baratrons (1, 10 & 1000 Torr) ($\pm$0.05% accuracy)
Thermometry	4 PRTs, Labfacility IEC 751 Class A

[a] Due to the non-linear response of MCT detectors to the detected radiation, all interferograms were Fourier transformed using Bruker's OPUS software with a non-linearity correction applied.

Table 2
Summary of the sample conditions for all measurements.

Temperature (K)	Initial CCl_4 pressure (Torr)[a]	Total pressure (Torr)	Spectral resolution (cm^{-1})[b]
208.0 ± 0.2	~0.20	7.501 ± 0.008	0.010
208.0 ± 0.2	~0.20	50.92 ± 0.15	0.015
207.9 ± 0.2	~0.20	99.32 ± 0.83	0.015
208.0 ± 0.3	~0.20	199.4 ± 0.2	0.030
207.9 ± 0.3	~0.20	348.5 ± 1.1	0.030
217.4 ± 0.3	0.505	7.523 ± 0.008	0.010
217.3 ± 0.3	0.495	51.44 ± 0.08	0.015
217.3 ± 0.3	0.495	99.95 ± 0.08	0.015
217.5 ± 0.3	0.505	199.5 ± 0.3	0.030
217.5 ± 0.3	0.505	399.2 ± 0.8	0.030
233.1 ± 0.3	0.830	7.501 ± 0.015	0.010
233.1 ± 0.2	0.830	49.92 ± 0.02	0.015
233.0 ± 0.2	0.750	99.78 ± 0.08	0.015
233.0 ± 0.2	0.784	201.5 ± 0.1	0.030
233.0 ± 0.2	0.750	401.5 ± 0.2	0.030
251.3 ± 0.2	0.810	7.501 ± 0.008	0.010
251.3 ± 0.2	0.742	50.86 ± 0.2	0.015
251.3 ± 0.2	0.723	199.7 ± 0.1	0.030
251.2 ± 0.2	0.737	400.2 ± 0.2	0.030
251.2 ± 0.2	0.780	600.6 ± 0.3	0.030
273.1 ± 0.2	0.606	7.538 ± 0.023	0.010
273.1 ± 0.2	0.716	172.9 ± 0.2	0.030
273.1 ± 0.2	0.717	351.5 ± 0.2	0.030
273.1 ± 0.2	0.717	759.2 ± 0.2	0.030
296.4 ± 0.5	0.809	350.5 ± 0.3	0.030
295.7 ± 0.5	0.679	760.0 ± 0.8	0.030

[a] MKS-690A Baratron readings are accurate to ±0.05%.
[b] Using the Bruker definition of 0.9/MOPD.

can be calculated from:

$$\mu^2_{\text{systematic}} = \mu^2_{\text{NIST}} + \mu^2_{\text{T}} + \mu^2_{\text{P}} + \mu^2_{\text{phot}}. \quad (2)$$

Note that using a NIST spectrum for intensity calibration effectively nullifies the errors in the CCl_4 partial pressures and cell pathlength, so these do not have to be included in Eq. (2). According to Eq. (2), the systematic error contribution, $\mu_{\text{systematic}}$, to the new cross sections is ~3%.

3.4. Comparison between absorption cross-section datasets

This section provides a comparison between the new dataset presented as part of this work and the older Nemtchinov dataset. This comparison will focus on the quality of the datasets in terms of their spectral resolution, signal-to-noise ratio, integrated band strength, wavenumber scale, and PT coverage. This new dataset is available electronically from the first author, and will be made available to the community via the HITRAN and GEISA databases. Preliminary retrievals from the ACE-FTS instrument using the new spectroscopic dataset are presented in Section 4.

3.4.1. Spectral resolution

All spectra used to create the Nemtchinov cross-section dataset were recorded at 0.03 cm^{-1} spectral resolution. While such a resolution is appropriate for high-pressure measurements, it leaves much of the fine structure unresolved when the total pressure of the sample mixture is low. This is well illustrated in Figs. 2 and 3, which compare selected spectral ranges of the new cross section at 208.0 K and 7.501 Torr with the Nemtchinov cross section at 207.9 K and 8.22 Torr. For the new measurements, resolutions between 0.01 and 0.03 cm^{-1} were used, depending on the total pressure of the mixture gas.

3.4.2. Signal-to-noise ratios (SNRs)

The SNRs of the new transmittance spectra, calculated using Bruker's OPUS software at ~840 cm^{-1} where the transmittance is close to 1, range from 800–1600 (rms). A direct comparison between the SNRs of the two absorption cross-section datasets is somewhat misleading because of the incorrectly chosen spectral resolution used for a number of Nemtchinov measurements. Whereas the SNRs are comparable for all the 0.03 cm^{-1} measurements, the new measurements at 0.01 cm^{-1} are noisier than the Nemtchinov measurements at 0.03 cm^{-1} by at most a factor of two. This has minimal impact for remote-sensing applications, however, given the overall high SNR of the new dataset.

3.4.3. Integrated band strengths

In order to compare integrated band strengths between datasets, integrals have been calculated over the spectral range of the Nemtchinov cross-section files, 750–812 cm^{-1}. This wavenumber range, however, does not extend far enough to obtain a true measure of the baseline position for comparison with the new dataset. Fig. 4 is a plot of integrated band strength (without error bars for clarity) against temperature for each dataset. The Nemtchinov integrated band strengths display a spread in values, likely resulting from baseline inconsistencies in these cross sections. The apparent temperature dependence in the new measurements is an artefact caused by the narrower spectral range of the integrals. When calculated over the range 700–860 cm^{-1}, integrated band strengths for the new cross sections correspond to 6.7163×10^{-17} cm molecule^{-1}, as given in Eq. (1), for all temperatures.

3.4.4. Wavenumber scale

As with other absorption cross-section datasets produced from the same laboratory, e.g. HFC-134a [27], CFC-12 [24], and HCFC-22 [28], the wavenumber scale for the Nemtchinov dataset is not accurate; it appears not to have been calibrated. The dataset presented in this work has been calibrated against the positions of isolated N_2O absorption lines in the HITRAN 2012 database [20]. The difference in wavenumber scales is illustrated in Figs. 2 and 3, which compare the new cross section at 208.0 K and 7.501 Torr with the Nemtchinov cross section at 207.9 K and 8.22 Torr. In this case the Nemtchinov cross section is shifted too low by ~0.010 cm^{-1} (a correction factor of ~1.000013).

3.4.5. Pressure–temperature coverage

An absorption cross-section dataset used in remote sensing should cover all possible combinations of pressure and temperature appropriate for the region of the atmosphere being observed; it is more accurate to interpolate between cross sections rather than extrapolate beyond them. Fig. 5 provides a graphical representation of the PT combinations for both datasets. It shows clearly that the

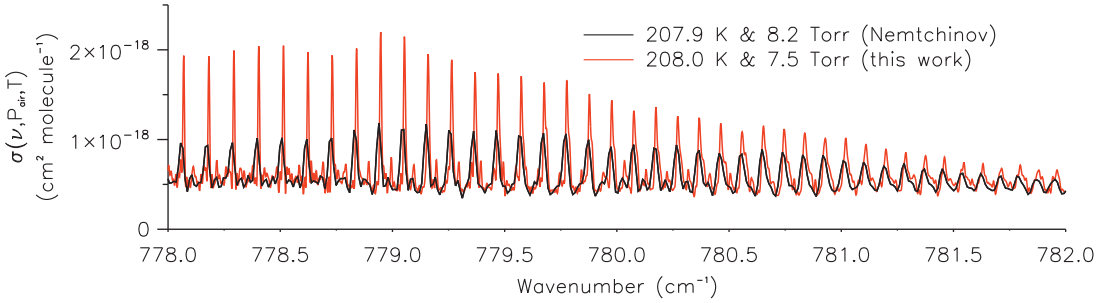

Fig. 2. The new IR absorption cross section of carbon tetrachloride/dry synthetic air (part of the $\nu_1 + \nu_4$ band) at 208.0 K and 7.501 Torr, with that of Nemtchinov [18] at 207.9 K and 8.22 Torr overlaid.

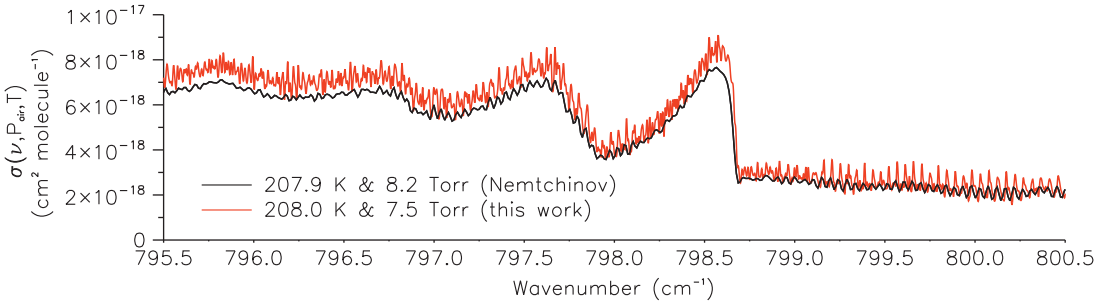

Fig. 3. The new IR absorption cross section of carbon tetrachloride/dry synthetic air (part of the ν_3 band) at 208.0 K and 7.501 Torr, with that of Nemtchinov [28] at 207.9 K and 8.22 Torr overlaid.

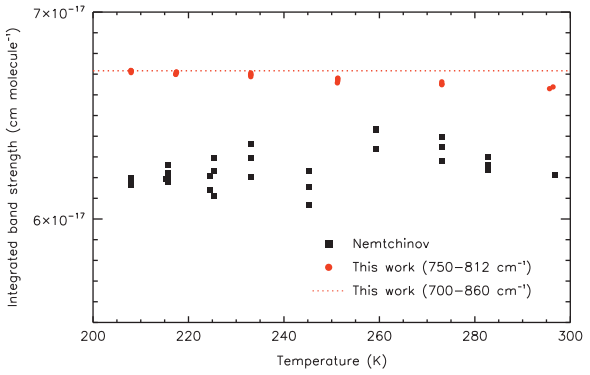

Fig. 4. A plot of integrated band strength versus temperature for each of the datasets over the wavenumber range 750–812 cm^{-1}. Also included for comparison is an indication of the integrated band strength over the range 700–860 cm^{-1} (this work), which is defined to be temperature independent.

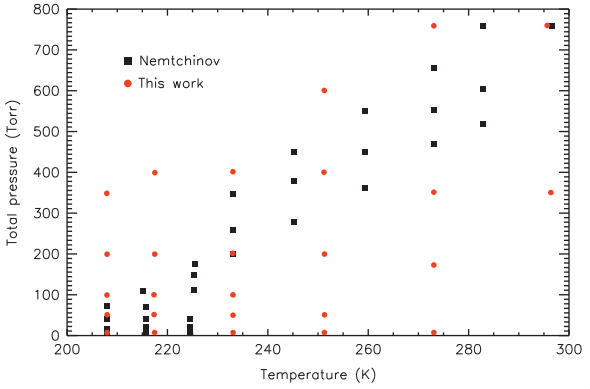

Fig. 5. A graphical representation of the PT coverage for both the new and Nemtchinov [18] datasets.

new dataset presented in this work greatly extends the PT coverage (26 PT combinations in total). Ideally, the dataset should cover temperatures down to 190 K; however, as noted by Nemtchinov and Varanasi [18], due to the sharp drop-off in CCl_4 vapour pressure below 208 K, it is not possible to record a spectrum below this temperature using a 26-cm-pathlength sample cell.

4. New ACE-FTS retrieval

As touched on in the Introduction, the ACE-FTS v3.0/v3.5 CCl_4 retrieval is biased high by up to ~20–30% relative to ground measurements. Note that the CCl_4 retrieval scheme is identical for the v3.0 and v3.5 datasets, the difference being in the meteorological data used as input for the pressure and temperature retrievals (the lowest ACE-FTS levels use these data directly). Due to an error in these inputs, v3.0 data should only be used for measurements taken until the end of September 2010, while v3.5 is valid for all ACE-FTS measurements. This section outlines an improved, preliminary ACE-FTS CCl_4 retrieval, which addresses the problem of the high bias. The retrieval is based on version 3.5 of the ACE-FTS retrieval software [29], with new CCl_4 spectroscopy (this work), updated microwindows, additional interfering species, and a new ILS [30] designed for the upcoming v4.0 processing. (The use of this new ILS, instead of that for v3.0/v3.5, reduces systematic errors in the retrieved VMRs arising from the ILS contributions to the residuals.)

The new microwindow set (listed in Table 3) consists of 35 microwindow 'slices' across the broad CCl_4 spectral feature, with a common set of baseline parameters (a scaling factor and a slope for the baseline are included in the least-squares analysis). These slices were chosen so as to avoid regions of bad spectral residuals, for instance near the 792 cm^{-1} Q branch of CO_2 (11101-10002 transition), which suffers from strong line mixing effects that the software is not currently equipped to calculate [6], and near numerous H_2O lines, where current spectroscopic line parameters are unable to provide the required accuracy. The altitude limits of the microwindows vary with latitude according to the phenomenological expression $\sin^2(\text{latitude}^\circ)$, to reflect the latitude dependence at lower altitudes of the saturation of spectral features in the microwindows, and at upper altitudes of the variation in CCl_4 abundance. An additional eight microwindows are included to improve the retrievals of various interferers, because the least-squares process can prematurely converge before reaching the optimal solution if the information content for one or more of the fitting parameters is too low.

The ACE-FTS v3.5 retrieval procedure has been explained previously [29]. In general, vertical VMR profiles of trace gases (along with temperature and pressure) are derived from the recorded transmittance spectra via a nonlinear least-squares global fit to the selected spectral region(s) for all measurements within the altitude range of

Table 3
Summary of the microwindows used in the new ACE-FTS CCl_4 retrieval.

Centre frequency (cm^{-1})	Microwindow width (cm^{-1})	Lower altitude (km)	Upper altitude (km)
772.17	0.38	$8-2\sin^2$(latitude°)	$30-5\sin^2$(latitude°)
773.53	0.70	$8-2\sin^2$(latitude°)	$30-5\sin^2$(latitude°)
780.10	0.40	$8-2\sin^2$(latitude°)	$30-5\sin^2$(latitude°)
780.77	0.30	$8-2\sin^2$(latitude°)	$30-5\sin^2$(latitude°)
781.26	0.32	$8-2\sin^2$(latitude°)	$30-5\sin^2$(latitude°)
785.99	0.34	$8-2\sin^2$(latitude°)	$30-5\sin^2$(latitude°)
787.41	0.34	$8-2\sin^2$(latitude°)	$30-5\sin^2$(latitude°)
788.85	0.38	$8-2\sin^2$(latitude°)	$30-5\sin^2$(latitude°)
793.20	0.60	$8-2\sin^2$(latitude°)	$30-5\sin^2$(latitude°)
793.80	0.36	$13-2\sin^2$(latitude°)	$30-5\sin^2$(latitude°)
794.81	0.90	$8-2\sin^2$(latitude°)	$30-5\sin^2$(latitude°)
795.90	0.80	$15-2\sin^2$(latitude°)	$30-5\sin^2$(latitude°)
796.60	0.40	$10-2\sin^2$(latitude°)	$30-5\sin^2$(latitude°)
797.23	0.26	$8-2\sin^2$(latitude°)	$30-5\sin^2$(latitude°)
797.55	0.30	$13-2\sin^2$(latitude°)	$30-5\sin^2$(latitude°)
797.84	0.20	$9-2\sin^2$(latitude°)	$11-2\sin^2$(latitude°)
797.95	0.30	$11-2\sin^2$(latitude°)	$30-5\sin^2$(latitude°)
798.27	0.30	$15-2\sin^2$(latitude°)	$30-5\sin^2$(latitude°)
798.75	0.30	$15-2\sin^2$(latitude°)	$30-5\sin^2$(latitude°)
799.05	0.30	$13-2\sin^2$(latitude°)	$30-5\sin^2$(latitude°)
799.54	0.32	$8-2\sin^2$(latitude°)	$30-5\sin^2$(latitude°)
800.53	0.50	$8-2\sin^2$(latitude°)	$30-5\sin^2$(latitude°)
801.05	0.34	$8-2\sin^2$(latitude°)	$30-5\sin^2$(latitude°)
801.32	0.24	$13-2\sin^2$(latitude°)	$30-5\sin^2$(latitude°)
801.83	0.26	$13-2\sin^2$(latitude°)	$30-5\sin^2$(latitude°)
802.15	0.30	$8-2\sin^2$(latitude°)	$30-5\sin^2$(latitude°)
802.56	0.28	$8-2\sin^2$(latitude°)	$30-5\sin^2$(latitude°)
802.83	0.26	$13-2\sin^2$(latitude°)	$30-5\sin^2$(latitude°)
803.52	0.44	$15-2\sin^2$(latitude°)	$30-5\sin^2$(latitude°)
805.10	0.32	$8-2\sin^2$(latitude°)	$30-5\sin^2$(latitude°)
807.26	0.40	$8-2\sin^2$(latitude°)	$30-5\sin^2$(latitude°)
808.95	0.30	$8-2\sin^2$(latitude°)	$30-5\sin^2$(latitude°)
809.65	0.30	$8-2\sin^2$(latitude°)	$30-5\sin^2$(latitude°)
810.30	0.40	$8-2\sin^2$(latitude°)	$30-5\sin^2$(latitude°)
811.19	0.26	$8-2\sin^2$(latitude°)	$30-5\sin^2$(latitude°)
806.25 [a]	1.10	$8-2\sin^2$(latitude°)	20
809.38 [b]	0.40	20	$30-5\sin^2$(latitude°)
829.03 [c]	0.50	10	20
1977.60 [d]	0.50	$9-3\sin^2$(latitude°)	21
1950.10 [e]	0.35	$12-4\sin^2$(latitude°)	$15-2\sin^2$(latitude°)
1986.09 [f]	0.30	$8-\sin^2$(latitude°)	22
2620.81 [g]	0.45	$8-2\sin^2$(latitude°)	20
2976.80 [h]	0.40	9	20

[a] Included to improve results for interferer $H_2{}^{16}O$.
[b] Included to improve results for interferer CO_2.
[c] Included to improve results for interferer HCFC-22.
[d] Included to improve results for interferer $H_2{}^{18}O$.
[e] Included to improve results for interferer $H_2{}^{16}O$.
[f] Included to improve results for interferer $H_2{}^{17}O$.
[g] Included to improve results for interferer $CO^{18}O$.
[h] Included to improve results for interferer C_2H_6.

interest. For the CCl_4 retrievals carried out for this work, the atmospheric pressure and temperature profiles and the tangent heights of the measurements were taken from the v3.5 processing of the ACE-FTS data. The abundances of most molecules with absorption features in the microwindows (see Table 4) were adjusted simultaneously with the CCl_4 VMR. A weak contribution for CFC-13 (CClF3), which is not listed in Table 4 as its VMR was not adjusted during the retrieval, was calculated based on abundances measured via in-situ studies. Spectroscopic line parameters and absorption cross sections for most molecules were taken from the HITRAN 2012 database [20], with the exception of HCFC-22 [28], CFC-113 [31], and $CHCl_3$ (PNNL). An ACE-FTS transmittance spectrum (from occultation ss8706) over the range 772–812 cm^{-1} is plotted in Fig. 6, along with several residual plots which provide an indication of the retrieval quality.

For the purposes of this work, a subset of 527 ACE-FTS occultations, covering March and April 2005 and providing a good coverage over all latitudes, was processed by the retrieval software. Fig. 7 is a plot of median VMR profiles in each of nine 20° latitude bins (from south to north, each bin contains 63, 64, 37, 45, 63, 74, 55, 69 and 57 profiles respectively); errors at each altitude are calculated as ± 1 MAD (median absolute deviation). Overlaid on each plot is the corresponding v3.0/v3.5 median profile (without error

Table 4
Summary of the molecules included in the microwindows for the new ACE-FTS CCl_4 retrieval.

Molecule	Lower altitude limit (km)	Upper altitude limit (km)	Nature of spectroscopic data
$ClONO_2$	$8-2\sin^2$(latitude°)	$30-5\sin^2$(latitude°)	Cross sections
$CHClF_2$ (HCFC-22)	$8-2\sin^2$(latitude°)	20	Cross sections
$C_2Cl_3F_3$ (CFC-113)	$8-2\sin^2$(latitude°)	20	Cross sections
$H_2{}^{16}O$	$8-2\sin^2$(latitude°)	$30-5\sin^2$(latitude°)	Line parameters
$H_2{}^{18}O$	$8-2\sin^2$(latitude°)	21	Line parameters
$C_2H_5ONO_2$ (PAN)	$8-2\sin^2$(latitude°)	20	Cross sections
HO_2NO_2	$8-2\sin^2$(latitude°)	$30-5\sin^2$(latitude°)	Cross sections
$H_2{}^{17}O$	$8-2\sin^2$(latitude°)	22	Line parameters
$^{12}C^{16}O_2$	$8-2\sin^2$(latitude°)	$30-5\sin^2$(latitude°)	Line parameters
$^{13}C^{16}O_2$	$8-2\sin^2$(latitude°)	$30-5\sin^2$(latitude°)	Line parameters
$^{12}C^{16}O^{18}O$	$8-2\sin^2$(latitude°)	20	Line parameters
O_3	$8-2\sin^2$(latitude°)	$30-5\sin^2$(latitude°)	Line parameters
NO_2	$8-2\sin^2$(latitude°)	20	Line parameters
HNO_3	$8-2\sin^2$(latitude°)	25	Line parameters
HCN	$8-2\sin^2$(latitude°)	$25-5\sin^2$(latitude°)	Line parameters
COF_2	$8-2\sin^2$(latitude°)	$30-5\sin^2$(latitude°)	Line parameters
$CHCl_3$	$8-2\sin^2$(latitude°)	20	Cross sections
C_2H_6	$8-2\sin^2$(latitude°)	20	Line parameters
C_2H_2	$8-2\sin^2$(latitude°)	21	Line parameters

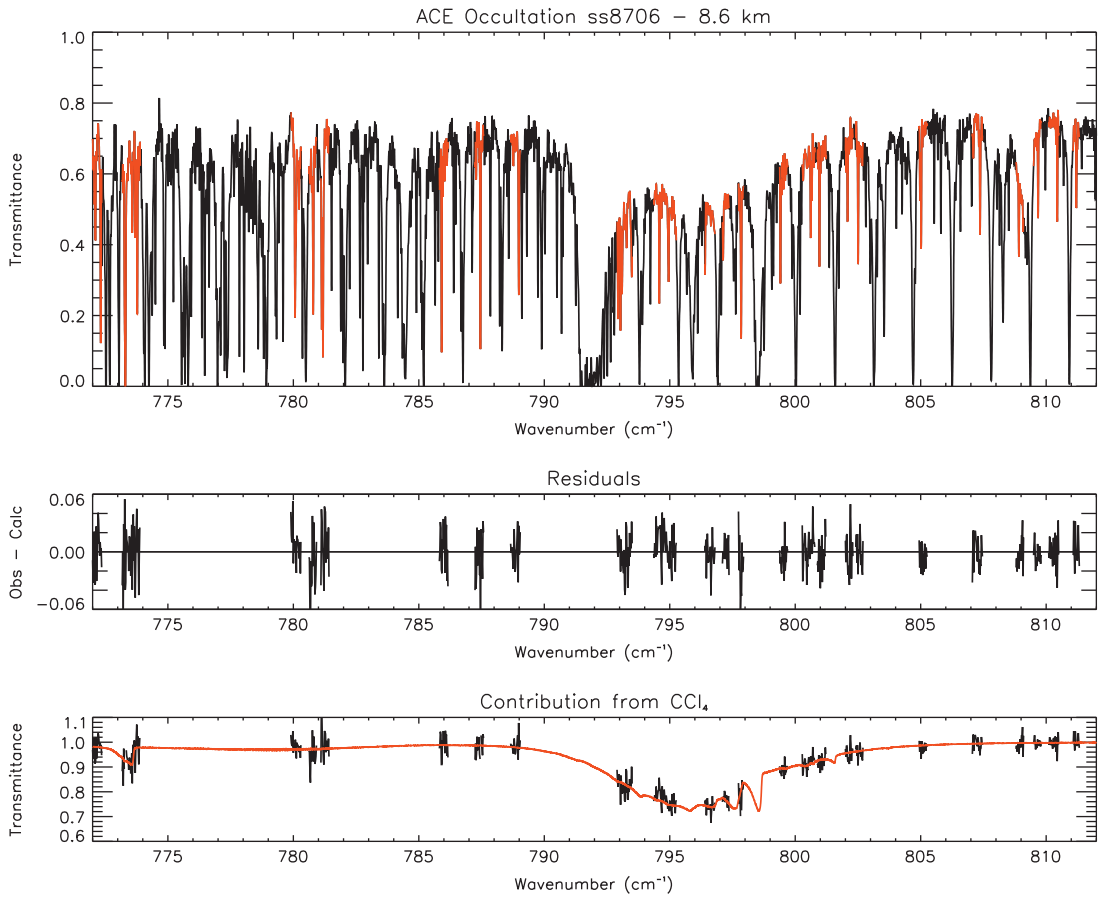

Fig. 6. Top panel: an ACE-FTS transmittance spectrum over the 772–812 cm^{-1} region for occultation ss8706 (recorded on 25 March 2005, off the coast of northern Scotland) at a tangent height of 8.60 km. The features in red represent the microwindows used in the new CCl_4 retrieval. Middle panel: the total observed – calculated residuals for the CCl_4 retrieval. Bottom panel: Observed/calculated ratio (without the inclusion of CCl_4 in the forward model), with the calculated CCl_4 transmittance contribution to the measurement overlaid. (For interpretation of the references to colour in this figure legend, the reader is referred to the web version of this article.)

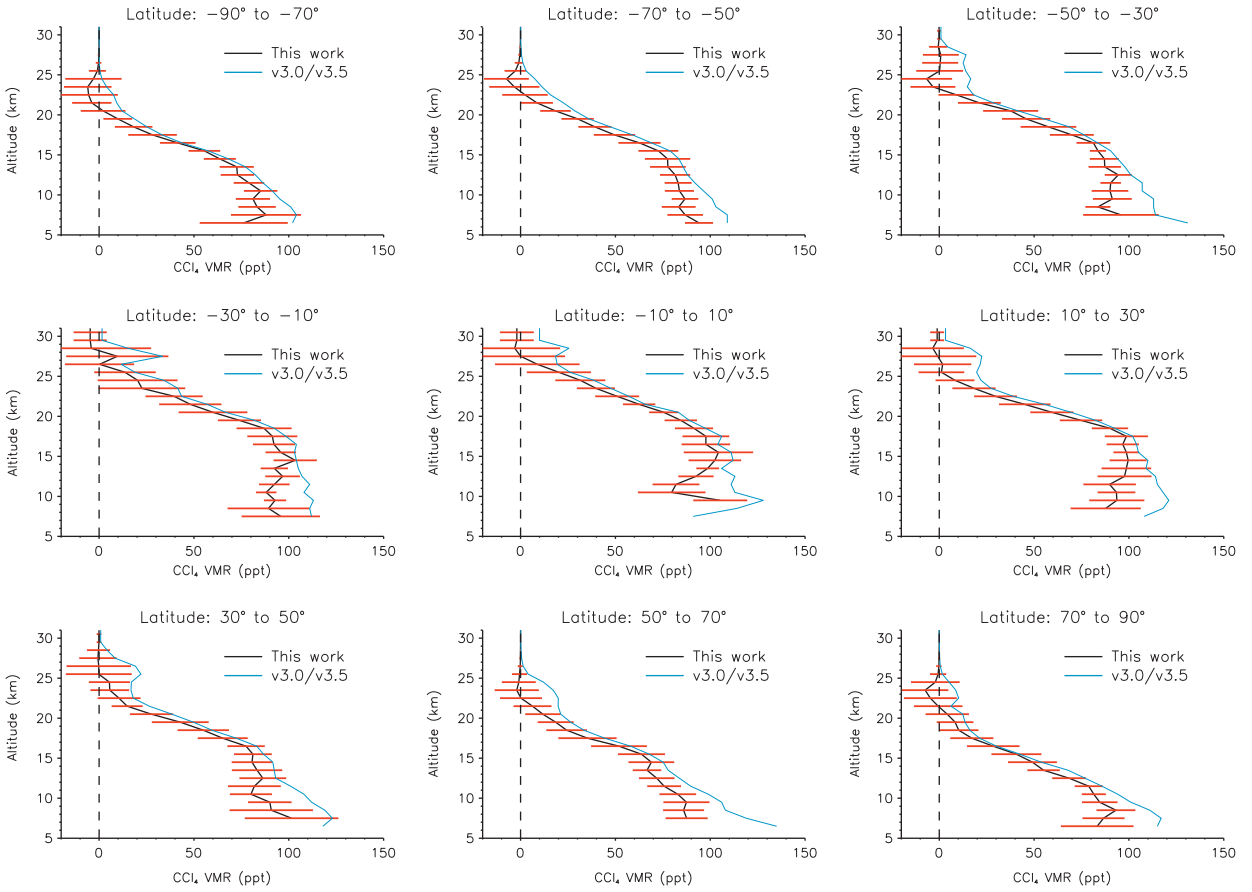

Fig. 7. A plot of median CCl_4 VMR profiles in nine 20° latitude bins from the new processing of a subset of 527 ACE-FTS occultations measured during March and April 2005 (in black). The errors at each altitude are calculated as ± 1 MAD (median absolute deviation). Overlaid on each plot is the corresponding v3.0/v3.5 median profile (in blue; without error bars for clarity) for the same occultations. (For interpretation of the references to colour in this figure legend, the reader is referred to the web version of this article.)

bars for clarity) for the same occultations. Unavoidably, by reducing the total wavenumber coverage of combined microwindows (the v3.0/v3.5 retrieval utilises a single CCl_4 microwindow of 787.50–805.50 cm^{-1}), the VMRs retrieved using the new scheme are noisier than was observed with v3.0/v3.5, however they are certainly more accurate; this accuracy can be assessed by comparison with ground measurements from early 2005. Based on data from the 2010 ozone assessment report [32], in particular Figure 1-1, mean global surface mixing ratios of CCl_4 at the time of the ACE-FTS measurements range from 92–95 ppt. With an atmospheric lifetime of 44 years [33] due to stratospheric loss, meaning that CCl_4 is well-mixed in the troposphere, these surface VMRs should be representative of those in the free troposphere. As shown by Fig. 7, these values compare well with retrieved ACE-FTS VMRs in the upper tropical troposphere (30°S and 30°N), where the air is relatively young. (Note that if the cross sections had been scaled using PNNL spectra, the retrieved VMRs would be on average 5.4% higher, and agreement with ground measurements worse.) However, there is an unphysical 'kink' in the upper tropospheric profile between 10°S and 10°N. It is possible that this is caused by strong water absorption contaminating the selected retrieval microwindows; water is typically much more abundant in the tropics compared to other regions. This will be investigated prior to the upcoming v4.0 processing.

The improvement in retrieval accuracy relative to v3.0/v3.5 can be attributed directly to the new cross sections and the changes made to the retrieval scheme. Disentangling the individual contributions to the systematic differences between profiles for the two schemes is beyond the scope of this work, however based purely on integrated band strengths the new CCl_4 cross sections lead to ~8% lower VMRs. It is likely that the new v4.0 ILS makes only a relatively small contribution of several percent to the improvement. The sizes of these systematic differences vary for different profiles, depending on, for example, the concentrations of interferers that are either missing from the forward model or represented by inadequate spectroscopy (in v3.0/v3.5), as well as the differences between the interpolated CCl_4 cross sections used for the two schemes. Since a number of the interferers inadequately characterised in the v3.0/v3.5 retrieval have larger concentrations in the troposphere, e.g. PAN which was not included in v3.0/v3.5, the systematic differences are larger in the troposphere.

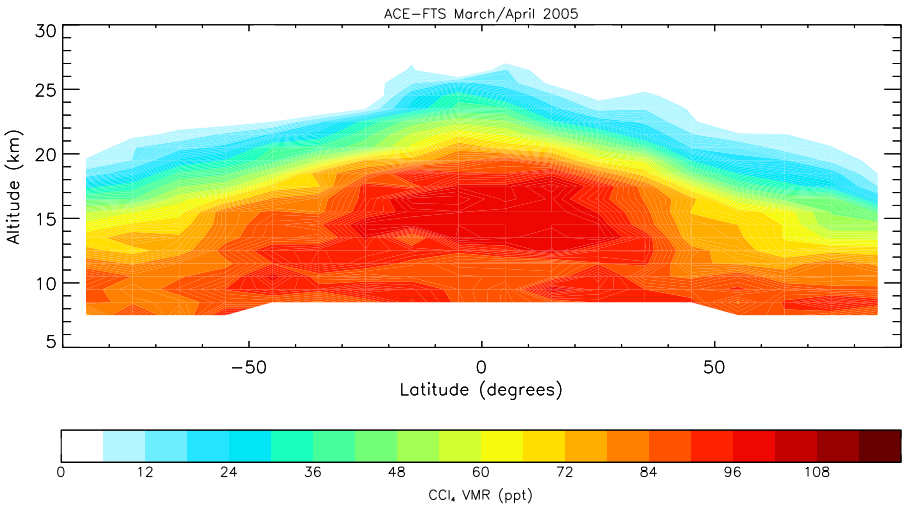

Fig. 8. A CCl_4 zonal median VMR cross-section plot for March/April 2005, constructed from 527 ACE-FTS VMR profiles assigned into 10° latitude bins.

Median profiles for the 527 ACE-FTS CCl_4 VMR profiles assigned into 10° latitude bins have been used to construct a CCl_4 zonal median VMR cross-section plot for March/April 2005 (Fig. 8); this provides an alternative means of viewing the data from Fig. 7. Those data points within the tropical troposphere (fewer than ten points in total) which deviate significantly from neighbouring values were removed and replaced by averages of these neighbouring VMRs. The plot in Fig. 8 illustrates clearly that CCl_4 VMRs decrease more rapidly with increasing altitude in the high-latitude/polar regions, reflecting the large-scale circulation of air around the globe, in which tropospheric air ascends into the stratosphere over the tropics and descends into the troposphere towards the poles.

The new retrieval scheme described in this work will form the basis for the CCl_4 retrieval in the upcoming processing version 4.0 of ACE-FTS data. This processing version will feature a new pressure and temperature retrieval, which will further improve the CCl_4 data product and provide more accurate trends.

5. Conclusions

New high-resolution IR absorption cross sections for air-broadened carbon tetrachloride have been determined over the spectral range 700–860 cm^{-1}, with an estimated uncertainty of ~3%. Spectra were recorded for mixtures of CCl_4 with dry synthetic air in a 26-cm-pathlength cell at spectral resolutions between 0.01 and 0.03 cm^{-1} (calculated as 0.9/MOPD) over a range of temperatures and pressures appropriate for upper troposphere – lower stratosphere conditions (7.5–760 Torr and 208–296 K). Intensities were calibrated against a CCl_4 spectrum in the NIST IR database. These new cross sections improve upon those currently available in the HITRAN and GEISA databases; namely they cover a wider range of pressures and temperatures, they have a more accurately calibrated wavenumber scale, they have more consistent integrated band intensities, and they were derived from spectra recorded at appropriate spectral resolutions.

It has been demonstrated that the new absorption cross sections, coupled with improvements in the microwindow selection, the addition of new interfering species, and a new ILS, lead to a more accurate ACE-FTS retrieval than v3.0/v3.5. It is important to note that the improvements made to the CCl_4 retrieval scheme arise predominantly from spectroscopic considerations. The revised CCl_4 absorption cross sections contribute about an 8% reduction in the bias relative to v3.0/v3.5 (based on a simple comparison of integrated band strengths). The rest of the bias has been reduced by the careful selection of microwindows based on sound spectroscopic judgement, and ensuring that spectral regions in which the line parameters of interfering species do not adequately calculate the measured ACE-FTS spectra are not included in the retrieval. A similar approach can be extended to CCl_4 retrievals from atmospheric IR spectra recorded by other remote-sensing instruments, e.g. MIPAS. The preliminary scheme outlined in this work will form the basis for the upcoming processing version 4.0 of ACE-FTS data.

Acknowledgements

We wish to thank the National Centre for Earth Observation (NCEO), funded by the UK Natural Environment Research Council (NERC), for supporting this work and for providing access to the Molecular Spectroscopy Facility (MSF) at the Rutherford Appleton Laboratory (RAL), as well as R.G. Williams and R.A. McPheat for providing technical support at the RAL. The ACE mission is funded primarily by the Canadian Space Agency.

References

[1] Allen NDC, Bernath PF, Boone CD, Chipperfield MP, Fu D, Manney GL, et al. Global carbon tetrachloride distributions obtained from the

Atmospheric Chemistry Experiment (ACE). Atmos Chem Phys 2009;9:7449–59. http://dx.doi.org/10.5194/acp-9-7449-2009.
[2] Myers RL. The 100 most important chemical compounds: a reference guide. Westport, Connecticut, United States of America: Greenwood Press; 2007.
[3] Liang Q, Newman PA, Daniel JS, Reimann S, Hall BD, Dutton G, et al. Constraining the carbon tetrachloride (CCl_4) budget using its global trend and inter-hemispheric gradient. Geophys Res Lett 2014;41:5307–15. http://dx.doi.org/10.1002/2014GL060754.
[4] Harris NRP, Wuebbles DJ, Daniel JS, Hu J, Kuijpers LJM, Law KS, et al. Scenarios and information for policymakers, chapter 5 in Scientific assessment of ozone depletion: 2014 (Global ozone research and monitoring project – report no. 55). Geneva, Switzerland: World Meteorological Organization; 2014.
[5] Carpenter LJ, Reimann S, Burkholder JB, Clerbaux C, Hall BD, Hossaini R, et al. Ozone-depleting substances (ODSs) and other gases of interest to the Montreal protocol, chapter 1 in Scientific assessment of ozone depletion: 2014 (Global ozone research and monitoring project – report no. 55). Geneva, Switzerland: World Meteorological Organization; 2014.
[6] Rinsland CP, Mahieu E, Demoulin P, Zander R, Servais C, Hartmann J-M. Decrease of the carbon tetrachloride (CCl_4) loading above Jungfraujoch, based on high resolution infrared solar spectra recorded between 1999 and 2011. J Quant Spectrosc Radiat Transf 2012;113:1322–9. http://dx.doi.org/10.1016/j.jqsrt.2012.02.016.
[7] Irion FW, Gunson MR, Toon GC, Chang AY, Eldering A, Mahieu E, et al. Atmospheric trace molecule spectroscopy (ATMOS) experiment version 3 data retrievals. Appl Opt 2002;41:6968–79.
[8] Zhou DK, Bingham GE, Anderson GP, Nadile RM. CIRRIS-1A measurements of stratospheric carbon tetrachloride (CCl_4) and carbon tetrafluoride (CF_4). Geophys Res Lett 1998;25:325–8.
[9] Cai S, Dudhia A. Analysis of new species retrieved from MIPAS. Ann Geophys 2014. http://dx.doi.org/10.4401/ag-6340.
[10] Brown AT, Chipperfield MP, Boone CD, Wilson C, Walker KA, Bernath PF. Trends in atmospheric halogen containing gases since 2004. J Quant Spectrosc Radiat Transf 2011;112:2552–66. http://dx.doi.org/10.1016/j.jqsrt.2011.07.005.
[11] Bernath PF, McElroy CT, Abrams MC, Boone CD, Butler M, Camy-Peyret C, et al. Atmospheric Chemistry Experiment (ACE): mission overview. Geophys Res Lett 2005;32:L15S01. http://dx.doi.org/10.1029/2005GL022386.
[12] Bernath PF. The Atmospheric Chemistry Experiment (ACE). J Quant Spectrosc Radiat Transf 2016 10.1016/j.jqsrt.2016.04.006, this issue.
[13] Chakraborty T, Verma AL. Vibrational spectra of CCl_4: isotopic components and hot bands. Part I Spectrochim Acta Part A: Mol Biomol Spectrosc 2002;58:1013–23.
[14] Rothman LS, Gamache RR, Goldman A, Brown LR, Toth RA, Pickett HM, et al. The HITRAN database: 1986 edition. Appl Opt 1987;26:4058–97.
[15] Massie ST, Goldman A, Murcray DG, Gille JC. Approximate absorption cross-sections of F12, F11, $ClONO_2$, N_2O_5, HNO_3, CCl_4, CF_4, F21, F113, F114, and HNO_4. Appl Opt 1985;24:3426–7.
[16] Orlando JJ, Tyndall GS, Huang A, Calvert JG. Temperature dependence of the infrared absorption cross sections of carbon tetrachloride. Geophys Res Lett 1992;19:1005–8.
[17] Rothman LS, Rinsland CP, Goldman A, Massie ST, Edwards DP, Flaud J-M, et al. The HITRAN molecular spectroscopic database and hawks (HITRAN atmospheric workstation): 1996 edition. J Quant Spectrosc Radiat Transf 1998;60:665–710.
[18] Nemtchinov V, Varanasi P. Thermal infrared absorption cross-sections of CCl_4 needed for atmospheric remote sensing. J Quant Spectrosc Radiat Transf 2003;82:473–81.
[19] Rothman LS, Barbe A, Benner DC, Brown LR, Camy-Peyret C, Carleer MR, et al. The HITRAN molecular spectroscopic database: edition of 2000 including updates through 2001. J Quant Spectrosc Radiat Transf 2003;82:5–44.
[20] Rothman LS, Gordon IE, Babikov Y, Barbe A, Benner DC, Bernath PF, et al. The HITRAN2012 molecular spectroscopic database. J Quant Spectrosc Radiat Transf 2013;130:4–50.
[21] Jacquinet-Husson N, Scott NA, Chédin A, Garceran K, Armante R, Chursin AA, et al. The 2003 edition of the GEISA/IASI spectroscopic database. J Quant Spectrosc Radiat Transf 2005;95:429–67.
[22] Jacquinet-Husson N, Crepeau L, Armante R, Boutammine C, Chédin A, Scott NA, et al. The 2009 edition of the GEISA spectroscopic database. J Quant Spectrosc Radiat Transf 2011;112:2395–445.
[23] Harrison JJ, Allen. NDC, Bernath PF. Infrared absorption cross sections for ethane (C_2H_6) in the 3 μm region. J Quant Spectrosc Radiat Transf 2010;111:357–63. http://dx.doi.org/10.1016/j.jqsrt.2009.09.010.
[24] Harrison JJ. New and improved infrared absorption cross sections for dichlorodifluoromethane (CFC-12). Atmos Meas Tech 2015;8:3197–207. http://dx.doi.org/10.5194/amt-8-3197-2015.
[25] Sharpe SW, Johnson TJ, Sams RL, Chu PM, Rhoderick GC, Johnson PA. Gas-phase databases for quantitative infrared spectroscopy. Appl Spectrosc 2004;58:1452–61.
[26] Chu PM, Guenther FR, Rhoderick GC, Lafferty WJ. The NIST quantitative infrared database. J Res Natl Inst Stand Technol 1999;104:59–81.
[27] Harrison JJ. Infrared absorption cross sections for 1,1,1,2-tetrafluoroethane. J Quant Spectrosc Radiat Transf 2015;151:210–6. http://dx.doi.org/10.1016/j.jqsrt.2014.09.023.
[28] Harrison JJ. New and improved infrared absorption cross sections for chlorodifluoromethane (HCFC-22). Atmos Meas Tech 2016. http://dx.doi.org/10.5194/amt-2015-389, in press.
[29] Boone CD, Walker KA, Bernath PF. Version 3 retrievals for the Atmospheric Chemistry Experiment Fourier transform spectrometer (ACE-FTS). In: Bernath PF, editor. The Atmospheric Chemistry Experiment ACE at 10: a solar occultation anthology. Hampton, Virginia, U.S.A.: A. Deepak Publishing; 2013. p. 103–27 Available at ⟨http://www.ace.uwaterloo.ca/publications/2013/Version3.5retrievals2013.pdf⟩.
[30] Boone CD, Bernath PF. Spectroscopic issues for the Atmospheric Chemistry Experiment (ACE). In: Proceedings of the 13th biennial HITRAN conference. Cambridge, Massachusetts, United States of America; 23 June 2014. ⟨http://dx.doi.org/10.5281/zenodo.11103⟩.
[31] Le Bris K, Pandharpurkar R, Strong K. Mid-infrared absorption cross-sections and temperature dependence of CFC-113. J Quant Spectrosc Radiat Transf 2011;112:1280–5.
[32] Montzka SA, Reimann S, Engel A, Krüger K, O'Doherty S, Sturges WT, et al. Ozone-depleting substances (ODSs) and related chemicals, chapter 1 in Scientific assessment of ozone depletion: 2010 (Global ozone research and monitoring project – report no. 52). Geneva, Switzerland: World Meteorological Organization; 2010.
[33] SPARC. Report on the lifetimes of stratospheric ozone-depleting substances, their replacements, and related species. In: Ko M, Newman P, Reimann S, Strahan S, editors. SPARC report No. 6, WCRP-15/2013; 2013.